# Comparison of Final Fracture Extraction Techniques for Interrupted *In situ* Tensile Tests of Glass Fiber Reinforced Polymers

Alexander Amirkhanov[1], Dietmar Salaberger[1], Johann Kastner[1], Christoph Heinzl[1], Eduard Gröller[2]

[1]University of Applied Sciences Upper Austria, Campus Wels, Austria

[2]Institute of Computer Graphics and Algorithms, TU Wien, Austria

## Abstract

To develop and optimize advanced composite materials such as glass fiber reinforced polymers (GFRPs) is an important topic for various application areas. To inspect mechanical properties of GFRPs, material engineers use interrupted in situ tensile tests. During these tests, a specimen is scanned multiple times in an industrial computed tomography (CT) device under increasing tensile loads, starting from no load until finally the fracture of the specimen occurs. In this work, we focus on the final step of the interrupted in situ tensile test, which is scanned when the specimen is completely losing its structural integrity in the final fracture zone. The defects occurring in the first loading stages merge and ultimately form the final fracture. For this reason, conventional techniques tend to generate error prone final fracture regions or surfaces and thus require more advanced algorithms for extraction. The main contribution of this paper is the comparison of different techniques for extracting the final fracture. In the comparison, we outline advantages and drawbacks of the presented techniques relative to each other.

**Keywords: feature extraction, final fracture extraction, interrupted in situ tensile tests**

## 1 Introduction

Currently, composite materials are intensively investigated and increasingly used in industrial applications. Composites are characterized by a light weight and outperform conventional materials such as steel, aluminum or plastic in various characteristics. This makes these materials especially interesting for automotive and aerospace industries. One of the promising composite materials is glass fiber reinforced polymers (GFRPs) consisting of glass fibers as reinforcement and a polymer matrix. The fibers provide stiffness and durability to the material while the matrix sticks the fibers together and prevents the material to fall apart. The manufacturers can produce GFRPs with different parameters (e.g., fiber content and orientation), which play a crucial role in material strength characteristics. To verify mechanical properties of GFRPs, manufacturers use destructive (e.g., microscopy) as well as nondestructive (e.g., ultrasonic methods, computed tomography) inspection techniques.

3D X-ray computed tomography (3DCT) is a nondestructive method that is widely used in inspection of industrial materials and components. The method makes use of the X-ray penetration to get information of the interior characteristics of the inspected object. A typical CT device consists of an X-ray tube, a rotary plate, and a detector (see Figure 1). The object to be scanned is placed on the rotary plate. During the 3DCT scanning, a stack of 2D attenuation images from the object in different angles is acquired. To obtain a 2D attenuation image, the rotary plate takes the required position and stops rotating. Then the X-ray tube beams X-rays though the object onto the detector. The attenuated X-rays hitting the detector are recorded and saved into an image file (2D attenuation image). When the scanning is finished, the stack of 2D attenuation images is reconstructed to a 3D volumetric image. The main advantage of 3DCT is that it allows characterizing the inside of the object in a relative short time. In addition, 3DCT allows monitoring dynamic processes like cooling/heating, drying or fracture processes in objects.

Interrupted in situ tensile testing is a method to investigate the damage mechanism in composite materials. During these tests, a specimen is placed in the in situ tensile stage (see Figure 1e), which allows applying user-specific loads to the specimen. The stage with the specimen inside is mounted in an industrial computed tomography (CT) device, in order to perform a series of consecutive CT scans under increasing load (Figure 2a: specimen scanned without load; Figure 2b: specimen scanned with the final fracture). After the interrupted in situ tensile test is completed, material engineers analyze the evolution of defects in the CT scans using specialized software tools [3]. As the final fracture determines the weakest part of the specimen, this region is especially interesting for the domain specialists. It contains important information about the damage mechanism and it allows domain specialists to deduce improvements of the material. For example, the shape of the final fracture changes in accordance to material properties such as fiber orientation or density. The Figure 3 illustrates two types of representations of the final fracture. The analysis of the final fracture poses various challenges. The first challenge is to define the borders of the final fracture. The defects occur in the whole specimen, but only certain defects are merging into the final fracture. To determine defects belonging to the final fracture is a challenging task even through a visual inspection by the domain specialists. The second challenge is finding a suitable representation of the final fracture. Physically, the final fracture has a 3D-shape. However, the definition of the final fracture as a 3D region in the CT scan has some disadvantages: for example, the thickness of the final fracture strongly depends on when the test was finished and how far the fracture is opened. Therefore, the thickness might change for different tests. In this work, we propose three new final fracture extraction pipelines (techniques). We compare these techniques with each other concerning different aspects, and provide advantages and disadvantages for each technique.
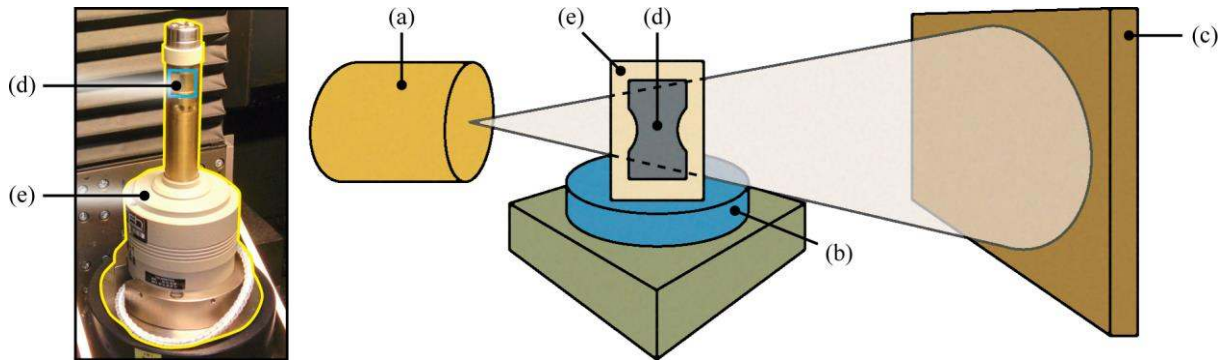
Figure 1: A typical CT device consists of the X-ray tube (a), the rotary plate (b), and the detector (c). In the case of interrupted in situ tensile tests, a test specimen (e) is placed in the tensile stage (d).

## 2 Workflow and Task Analysis

Interrupted in situ tensile testing coupled with CT is a relatively new topic. Due to this reason, there is a lack of purpose developed tools in the field. Commercially available tools such as VGStudio [1] or Avizo [2] do not provide the required functionality. In this work, we take as a basis the 4DCT tool developed by Amirkhanov [3] et al. The tool was especially designed to analyze the results of interrupted in situ tensile tests. It provides a rich functionality such as automatic defect classification, defect visualization, defect density map visualization as well as final fracture surface extraction and visualization. In analyzing the results of interrupted in situ tensile tests, material engineers are especially interested in the extraction of the final fracture zone. They want to extract the region as precise as possible using a reliable approach. In this work, we have extended the tool with three additional final fracture extraction pipelines. Hereinafter, we will refer the original pipeline as P1, and new pipelines as P2, P3, and P4 (see Figure 4). Pipelines P1, P2 and P3 were designed to extract the central region of the final fracture, and P4 was designed to extract the whole extent of the final fracture. We have done a comparison of all presented pipelines in which we outline their advantages and disadvantages. However, due to the fact that P4 has a different application scenario than the other pipelines we do not make a direct comparison of this pipeline with the others. All the pipelines require a binary mask of defects to generate the results. The pipelines work in the following way:

- P1: This pipeline is using a line profiling approach, P1 calculates a surface model of the final fracture (see Figure 3a). The profiling lines are oriented along the force direction. For each line, the medium position of all intersected defects is calculated. Then, the medium points of all lines are used to construct a surface, which is smoothed afterward to remove the noise.
- P2: This pipeline is similar to P1 excluding the last smoothing step. This pipeline represents the final fracture as a surface (see Figure 3b).
- P3: This pipeline calculates a final fracture surface out of a 3D-region (see Figure 3c). P3 uses the line profiling step as described in P1 to extract the final fracture surface.
- P4: This pipeline represents the final fracture as a 3D-region in the form of a segmented mask (see Figure 3d). To compute the region a sequence of filters is applied. First, a low-pass filter is applied to calculate a defect density map. Then Otsu's threshold method is used to extract the region of the final fracture.

In this work, we use a CT scan of a test specimen under the load of 330 newtons performed on a GE phoenix|xray nanotom device to illustrate and results of all the final fracture extraction pipelines. More detailed information about the CT device and scanning parameters can be found in [3] and [19].
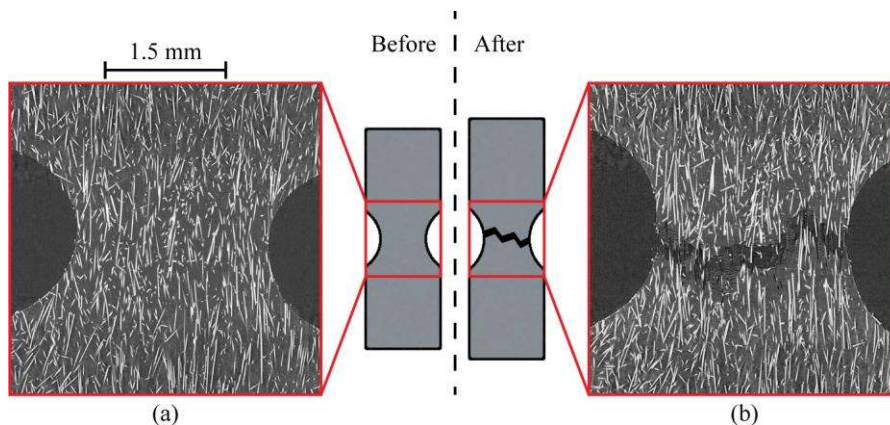


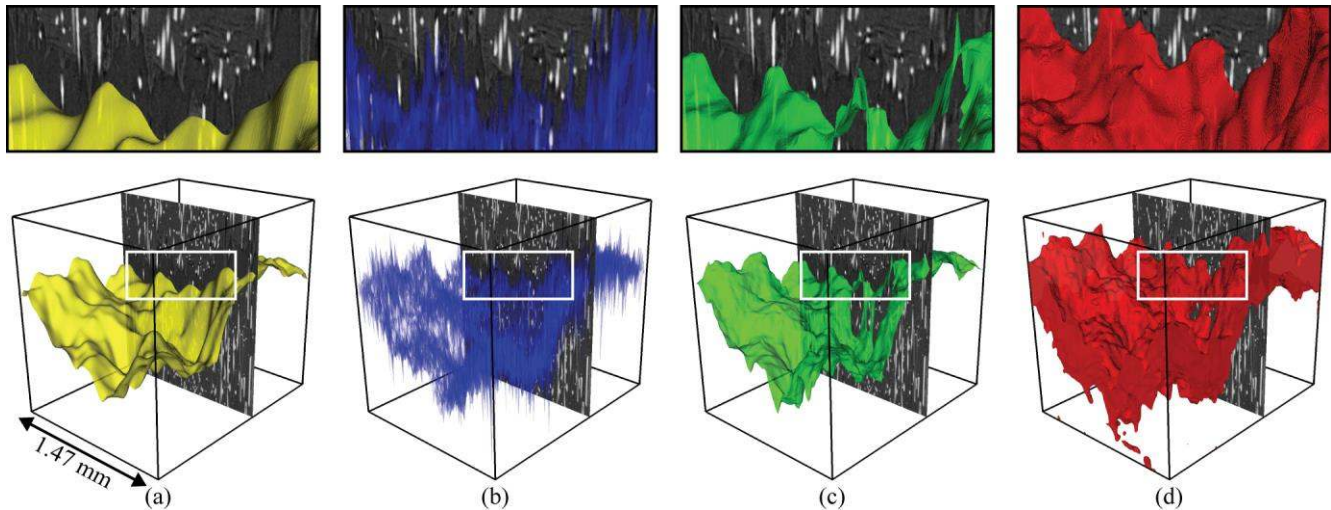Figure 2: A test specimen before (a) and after (b) breakage.

Figure 3: Comparison of four final fracture extraction pipelines. Pipelines P1 (a), P2 (b), P3 (c) represent the final fracture as a surface while P4 (d) represents the final fracture as a 3D-region.

## 3 Related work

Visualization of fiber reinforced composites: Fritz et al. [4] presented a method for visual analysis and characterization of graphite particles in ductile iron and steel fiber in reinforced sprayed concrete. Weissenböck et al. [5] developed the FiberScout tool for analysis of fiber characteristics in fiber reinforced polymers. For visualization and interactive exploration of fiber characteristics, the FiberScout uses a direct volume rendering and various histograms techniques such as scatter plots, parallel coordinates, and polar coordinates. However, these techniques are targeted on analyzing a single CT image, which makes it difficult to apply the tools to analyze results of interrupted in situ tensile tests.

Visualization of time-varying data: Aigner et al. [5] provided an overview of time-oriented visualizations techniques for many application domains. Havre at al. presented the ThemeRiver [6] technique for visualization of an evolution of thematic variations over time. Byron et al. [6] presented similar approach Stracked Graphs. Waser et al. [7] presented the World Lines visualization to assist exploring alternative scenarios and decision making for multiple heterogeneous simulation runs. Bajaj at al. [8] presented the hypervolume visualization technique to provide explanatory images of n-dimensional scalar fields. Lui et al. [9] presented a data mining methods for time-series data. All these methods were designed to work with many different applications scenarios, however none of them is directly working with CT data.

CT in the medical domain: Gorbunova et. al. [10] presented a method for registration 4D-CT lung datasets. The method uses intensity information together with geometrical features such as surfaces and curves extracted of CT data. McGary [11] presented a method for real-time tumor tracking in external beam radiotherapy. Van Pelt et. al. [12] presented a framework for pre-clinical cardiovascular research. The tool allows the user to interactively explore the 4D blood-flow data and depict the essential blood-flow characteristics. In these works, attention is manly focused on developing precise registration techniques and tracking specific features like blood-flow. Due to specific of the domain field, these methods cannot be directly applied for analysis industrial CT data.

Segmentation and feature extraction: Landstrom et al. [13] presented an automatic system to detect cracks in steel slabs based on their morphology. Fujita et al [14] presented two preprocessing techniques to reduce noise like irregularities, illuminated conditions, and shading for future crack detection. Oliveira [15] presented an integrated system to detect and characterize cracks in road pavement surface. Papaodysseus et al. [17] presented a segmentation method and a pattern analysis to reconstruct ancient wall paintings. Li et al. [18] presented an approach to segment tubular structures, e.g. vessels. To overcome certain limitations, they used 4D-curves instead of 3D ones to represent tabular structures. Reh et al. [16] presented a tool for evaluating and analysis of 4DCT datasets. All the techniques mentioned above are focused on specific application scenarios and cannot be used to extract the final fracture zone without any adaptions. Amirkhanov at al. [3] presented a tool, which can automatically extract the final fracture zone from CT scans of GFRPs. In this paper, we refer the final fracture extraction technique of Amirkhanov et al. [3] as P1 and we compare this technique with the three new presented methods.
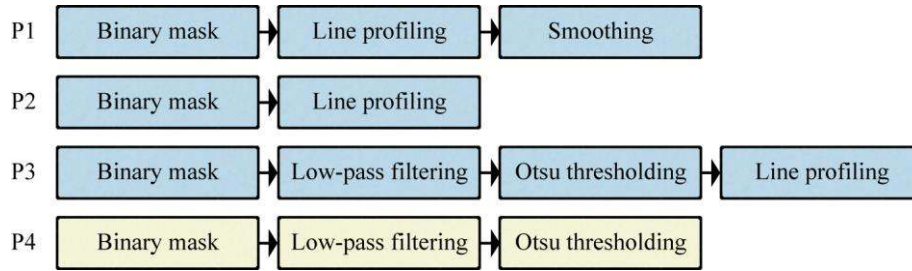
Figure 4: Four pipelines to extract the final fracture. Pipelines highlighted by a blue color are designed to extract the central region of the final fracture. Pipeline P4 is highlighted by a yellow color is designed to extract the whole extent of the fracture region.

## 4 Results

As expected, all the pipelines provide different results. Table 1 shows a comparison between presented final fracture extraction pipelines. The choice of a pipeline to use strongly depends on the user requirements. For example, if the user needs to extract the whole extent of the final fracture region, the choice towards P4 has to be done. The final fracture extracted using P4 is represented as a region and thus using this representation the user can distinguish defects belonging to the final fracture from thus defects, which are outside of the final fracture. Another advantage of P4 is that the final fracture region is realistically represented where all important features are kept such as volume and shape. Pipelines P1, P2, and P3 should be used when the user needs to extract the central region of the final fracture. Typically, results obtained using P2 for the real data have a high level of noise (see Figure 6). Therefore, we recommend using P2 only in cases when the data quality is high enough in terms of contrast, artifacts and noise. Pipelines P1 and P3 show similar results, but there are two major differences. The first difference is that P1 uses the whole binary image to calculate the surface, while P3 uses only high density regions. In the result, the representation of P1, in contrast to P3, has no holes in thin regions (see Figure 3). The second difference is that P1 makes the result surface more flat with increasing the smoothing coefficient (hillocks lower and hollows less deep, see **Error! Reference source not found.**). This due to P1 uses smoothing on the last step, which average the surface vertexes.

| Name | Description | Advantages and disadvantages |
|------|-------------|------------------------------|
| P1 | The final fracture is represented as a surface. This pipeline can calculate the approximate fracture surface even in thin regions. This is possible because, this technique uses the whole binary image but not only high defect density regions. The technique requires a smoothing to get rid of the noise in the surface. | + High level of abstraction<br>- Parameters are required to smooth the surface |
| P2 | The final fracture is represented as a surface. This pipeline is similar to P1 excluding the last smoothing step. The pipeline does not require any parameters to be performed. | + High level of abstraction<br>+ No parameters are required to calculate the surface<br>- Noisy surface |
| P3 | The final fracture is represented as a surface. In thin regions of the final fracture holes are possible in the result surface. The technique requires parameters in the low-pass filtering step to calculate the defect density map. | + High level of abstraction<br>+ No smoothing of the surface is required<br>- In thin regions of the final fracture surface cannot be extracted<br>- Parameters are required to calculate the defect density map |
| P4 | The final fracture is represented as a 3D-region. Though the region quite precisely outlines the final fracture, the representation has a low level of abstraction. That means the representation encodes parameters such as the fracture thickness, which can vary from one experiment to another one. The technique requires parameters to calculate a defect density map. | + Realistic representation of the final fracture<br>- Low level of abstraction<br>- Parameters are required to calculate the defect density map |

Table 1 Comparison of the final fracture extraction pipelines.

The most crucial step in terms of the results for pipelines P1 and P3 is smoothing. To perform the smoothing operator, we use Gaussian blurring. This filter only uses a single parameter: variance. The variance determines the size of the Gaussian kernel and it can be defined either in pixels or in units (e.g., micrometers). **Error! Reference source not found.** shows how different parameters settings influence the result surfaces. For P1 increasing the variance decreases the level of details of the surface and **Error! Reference source not found.** changes the surface (makes it more flat), while for P3 increasing the variance only decreases the level of details of the surface. Therefore, we conclude, that P3 provides results, which less influenced by parameters settings. Figure 6 shows superposition visualizations of all possible pairs of final fracture surfaces extracted using pipelines P1, P2, and P3. The top view shows that the surface extracted using P2 has a uniformly distributed noise in comparison to surfaces extracted using P1 and P3; and the surface extracted using P1 has less deep hollows than the surface extracted using P3. The frontal view
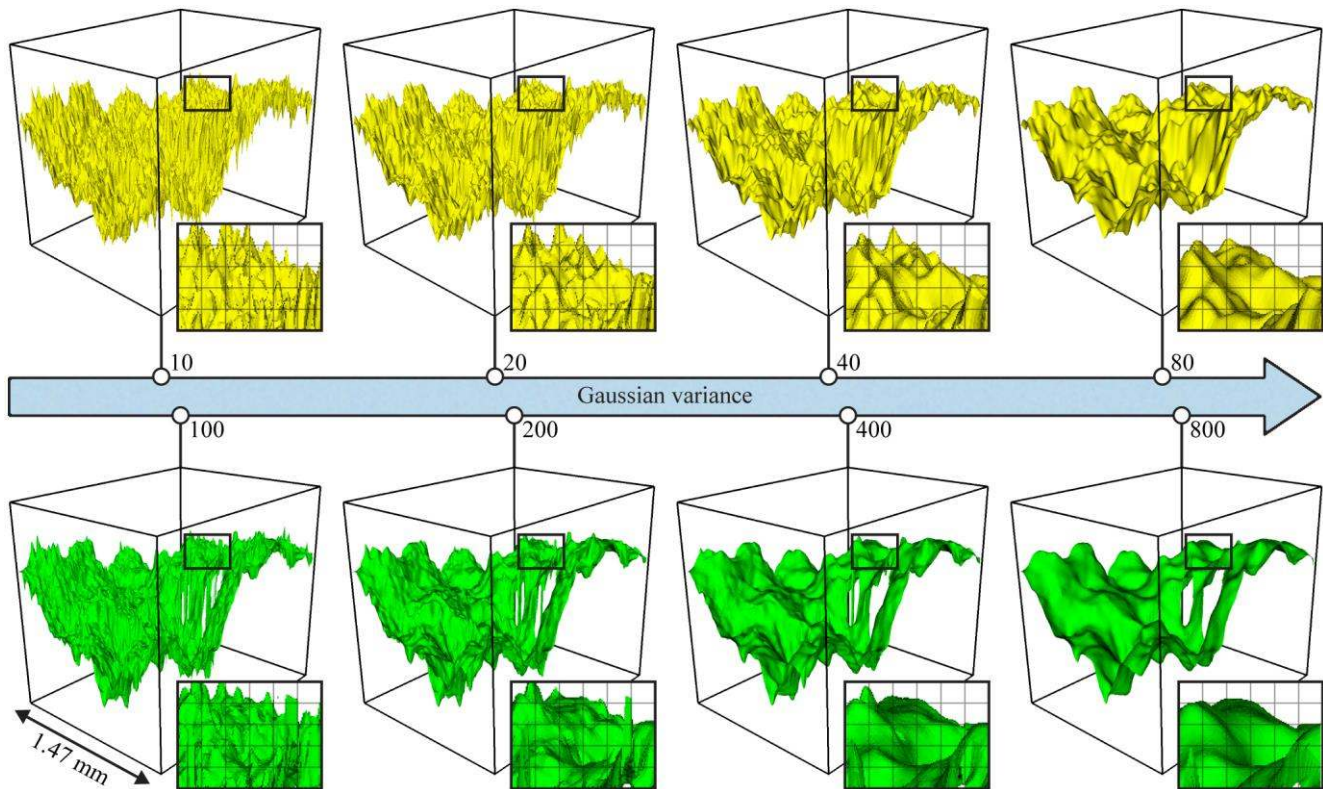
Figure 5: Influence of the Gaussian blurring parameters on the result surfaces of pipelines P1 and P3. For each surface, Gaussian blurring was applied different variance. Both pipelines show that with increasing the variance parameter, level of details is decreased. However, with decreasing level of details of P1 makes the surface flat while P3 preserves the relief.

shows the level of noise in the surface extracted using P1; and that the surface extracted using P3 has higher hillocks than the surface extracted using P1.

## 5 Conclusions

We have presented three new additional pipelines for extraction of the final fracture in GFRPs from CT volumetric images. Two of these techniques extract the final fracture as a surface and the one extracts the final fracture as a volumetric extent. We made a comparison of all the pipelines available in the tool and outlined advantages and disadvantages of each pipeline. We provided recommendations in which situations which pipeline the user should use. In addition, we performed an analysis how the Gaussian variance parameter in the smoothing step (using Gaussian blurring) influences on results of P1 and P3. In the analysis, we found out that with increasing the variance level of details is decreased in both surfaces. However, with the increasing the parameter P1 tends to make surface flat, while P3 preserves the relief.
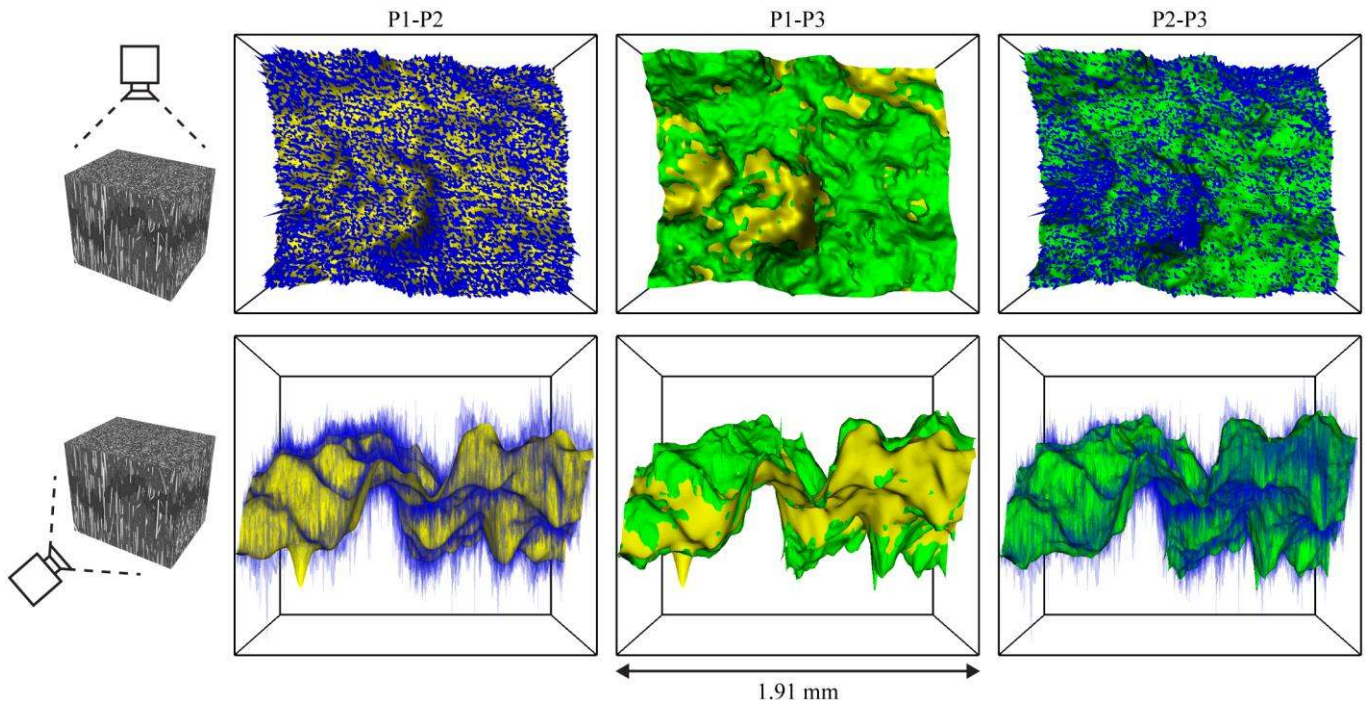
Figure 6: A pairwise comparison of pipelines P1 (yellow), P2 (blue), and P3 (green) from top-down view. P2 in comparison to P1 and P3 shows a high level of noise in the fracture surface. P1 in comparison to P3 has less deep hollows (in the hollow regions the yellow surface is visible). This is due to P1 uses a smoothing step to reduce noise in the surface which make it more flat as well.

## Acknowledgements

## References

[1]     VGStudio Max: basic functionality. http://www.volumegraphics.com/en/products/vgstudio-max/basic-functionality/. Accessed: 2016-03-07.

[2]     Avizo 3d software. http://www.fei.com/software/avizo3d/. Accessed: 2016-03-07.

[3]     A. Amirkhanov, A. Amirkhanov, D. Salaberger, J. Kastner, E. Gröller, and C. Heinzl (2016), Visual Analysis of Defects in Glass Fiber Reinforced Polymers for 4DCT Interrupted In situ Tests. Computer Graphics Forum, 35: 201–210. doi:10.1111/cgf.12896.

[4]     L. Fritz, M. Hadwiger, G. Geier, G. Pittino, E. Gröller, A visual approach to efficient analysis and quantification of ductile iron and reinforced sprayed concrete.IEEE Trans Vis Comput Graph 2009;15(6):1343–50. http://dx.doi.org/10.1109/TVCG.2009.115.

[5]     J. Weissenböck, A. Amirkhanov, W. Li, A. Reh, A. Amirkhanov, E. Gröller, et al. FiberScout: an interactive tool for exploring and analyzing fiber reinforcedpolymers. In: IEEE pacific visualization, 2014. p. 153–60.

[6]     L. Byron, M. Wattenberg. Stacked graphs – geometry & aesthetics. IEEE Trans VisComput Graph 2008;14(6):1245–52. http://dx.doi.org/10.1109/TVCG.2008.166.

[7]     J. Waser, R. Fuchs, H. Ribičić , B. Schindler, G. Blöschl, E. Gröller. World lines. IEEETrans Vis Comput Graph 2010;16(6):1458–67.

[8]     C. Bajaj, V. Pascucci, G. Rabbiolo, D. Schikore, Hypervolume visualization: achallenge in simplicity. In: IEEE symposium on volume visualization (CatNo989EX300), 1998. http://dx.doi.org/10.1109/SVV.1998.729590.

[9]     LM. Lui, J. William, Data mining on time series: an illustrative using fast foodfranchise data. Computational Statistics & Data Analysis 2001;37:455–76.

[10]    V. Gorbunova, S. Durrleman, P. Lo, X. Pennec and M. de Bruijne, "Lung CT registration combining intensity, curves and surfaces," 2010 IEEE International Symposium on Biomedical Imaging: From Nano to Macro, Rotterdam, 2010, pp. 340-343. doi: 10.1109/ISBI.2010.5490341

[11]    J. McGary, Real-Time Tumor Tracking for Four-Dimensional Computed Tomography Using SQUID Magnetometers IEEE Transactions on Magnetics, 2009, 45, 3351-3361

[12]    R. van Pelt, J. Olivan Bescos, M. Breeuwer, R. Clough, E. Gröller, B. ter Haar Romenij, et al. Exploration of 4D MRI blood flow using stylistic visualization. IEEE Trans Vis Comput Graph 2010;16(6):1339–47. http://dx.doi.org/10.1109/TVCG.2010.153.

[13]   A. Landstrom and M. J. Thurley, "Morphology-Based Crack Detection for Steel Slabs," in IEEE Journal of Selected Topics in Signal Processing, vol. 6, no. 7, pp. 866-875, Nov. 2012.
doi: 10.1109/JSTSP.2012.2212416

[14]   Y. Fujita, Y. Mitani and Y. Hamamoto, "A Method for Crack Detection on a Concrete Structure," 18th International Conference on Pattern Recognition (ICPR'06), Hong Kong, 2006, pp. 901-904.
doi: 10.1109/ICPR.2006.98

[15]   H. Oliveira and P. L. Correia, "Automatic Road Crack Detection and Characterization," in IEEE Transactions on Intelligent Transportation Systems, vol. 14, no. 1, pp. 155-168, March 2013.
doi: 10.1109/TITS.2012.2208630

[16]   A. Reh, A. Amirkhanov, J. Kastner, E. Gröller, C. Heinzl: Fuzzy feature tracking: Visual analysis of industrial 4d-xct data. Computers & Graphics 53, Part B (2015), 177 – 184. 4

[17]   C. Papaodysseus, M. Exarhos, M. Panagopoulos, P. Rousopoulos, C. Triantafillou and T. Panagopoulos, "Image and Pattern Analysis of 1650 B.C. Wall Paintings and Reconstruction," in IEEE Transactions on Systems, Man, and Cybernetics - Part A: Systems and Humans, vol. 38, no. 4, pp. 958-965, July 2008.
doi: 10.1109/TSMCA.2008.923078

[18]   H. Li and A. Yezzi, "Vessels as 4-D Curves: Global Minimal 4-D Paths to Extract 3-D Tubular Surfaces and Centerlines," in IEEE Transactions on Medical Imaging, vol. 26, no. 9, pp. 1213-1223, Sept. 2007.
doi: 10.1109/TMI.2007.903696

[19]   G. Rao, A. Amirkhanov, D. Salaberger, C. Heinzl, J. Kastner, Damage characterization in SFRP using X-ray computed tomography after application of incremental and interrupted in situ quasi static tensile loading, in Industrial Computed Tomography, Leuven, 2017